processes

MDPI

Article

Stress State and Fatigue Life Assessment of the Bolts at the Outlet End of Fracturing Pump

Haibo Liu [1], Xiaogang Wang [1], Yuanyuan Wang [1], Xian Shi [1], Wang Tian [1], Bingsheng Wang [1] and Rui Sun [2,*]

[1] Technology Inspection Center of Shengli Oilfield, SINOPEC, Dongying 257061, China; liuhaibo330.slyt@sinopec.com (H.L.); wangbingsheng.slyt@sinopec.com (B.W.)
[2] College of Mechanical and Automotive Engineering, Qingdao University of Technology, Qingdao 266520, China
* Correspondence: sunrui_92@126.com

Abstract: The fracturing pump serves as a critical piece of equipment in enhancing oil and gas recovery rates. However, under the coupled action of high-pressure fluid pulsation circulation in the pump body and the vibration of fracturing equipment, the bolts connecting the fracturing pump and fracturing manifold flange are prone to fatigue failure. In this paper, a three-dimensional finite-element model of the threaded bolt connection structure at the fracturing pump outlet end with a fine thread structure was established, and the measured vibrational displacement of the fracturing pump under different driven modes was used as the load to obtain the internal stress state of the full-thread bolt and the double-headed bolt used in the fracturing operation site. Based on the stress state, the fatigue life of the two types of bolts under various loading conditions was then simulated using the Brown—Miller fatigue damage criterion. The results indicate that for bolts of the same structural type, the maximum stress and stress variation amplitude increase in the sequence of the diesel-driven, single-motor-driven, and dual-motor-driven methods. Additionally, under the same load, the stress of the full-thread bolt is lower than that of double-headed bolt. The fatigue life analysis results show that under the vibrational load of diesel drive, the full-thread bolt can obtain a longer fatigue life of approximately 2042.89 h. However, under the load of dual-motor-driven method, the fatigue life of double-headed bolt is the lowest, only 717.46 h. A comparison with the fatigue life of bolts in actual engineering projects indicates that the predicted fatigue life of the bolts is consistent with the actual service life, which can provide effective guidance for the inspection and maintenance of fracturing pump equipment.

Keywords: stress state; fatigue life; bolts; vibrational displacement; fracturing pump

check for updates

Academic Editor: Sara Liparoti

Received: 25 December 2024
Revised: 15 January 2025
Accepted: 24 January 2025
Published: 27 January 2025

Citation: Liu, H.; Wang, X.; Wang, Y.; Shi, X.; Tian, W.; Wang, B.; Sun, R. Stress State and Fatigue Life Assessment of the Bolts at the Outlet End of Fracturing Pump. *Processes* **2025**, *13*, 355. https://doi.org/10.3390/pr13020355

Copyright: © 2025 by the authors. Licensee MDPI, Basel, Switzerland. This article is an open access article distributed under the terms and conditions of the Creative Commons Attribution (CC BY) license (https://creativecommons.org/licenses/by/4.0/).

1. Introduction

Hydraulic fracturing technology is a critical method for the efficient development of oil and gas fields, enhancing recovery rates in low-permeability reservoirs and extracting unconventional hydrocarbons [1,2]. In recent years, hydraulic fracturing technology has been extensively adopted and applied in the extraction of shale oil. The fracturing pump is one of the crucial devices in the hydraulic fracturing operation process of oil and gas fields. The reliability of the fracturing pump equipment will be directly associated with the safety of the fracturing operation and the efficiency of oil and gas exploitation. To accommodate the requirements of complex reservoirs, low-permeability oil and gas fields, and unconventional oil and gas resources, the operation of fracturing pumps is progressively evolving towards higher pressure and larger displacement [3,4]. Under the coupled effect

of the high-pressure fluid pulsating circulation within the pump body and the vibration of the fracturing equipment, the bolts at the flange connection between the fracturing pump and the fracturing manifold have been enduring a complex variable stress at a relatively high level for an extended period. They are highly susceptible to fatigue fracture, which severely impacts the safe operation of the fracturing operation and the implementation efficiency of oil and gas field exploitation.

In fact, due to the inherent operating characteristics of the fracturing pump, its internal components and those connected to it experience varying degrees of alternating cyclic loads [5]. Therefore, the fatigue failure of the relevant components of the fracturing pump during the fracturing operation process is particularly prominent [6]. At present, researchers have carried out extensive studies on the fatigue damage phenomena of each component in the fracturing pump equipment. Wei et al. employed the bilinear cohesive zone model to predict the fatigue crack growth of the fracturing pump head, and their research indicated that the initial crack size and the diameter ratio of cross bore on the pump head have significant effects on the fatigue crack growth behaviors along the crack front; under such conditions, the fatigue crack growth rates at the crack front are periodic [7]. Zhang and Zhou et al. tackled the issue of fatigue cracking in the pump head body of fracturing pumps by constructing an analysis model for the cracked pump head body using the finite-element method and identified both the initiation point and the root cause of the fatigue cracking [8]. Hu evaluated the fatigue crack expansion rate in fluid cylinder of the fracturing pump experimentally and established a finite-element model to predict the fatigue life of the fluid cylinder of the fracturing pump, and the accelerating effect of corrosion on fatigue crack propagation is also considered in the analysis [9].

As a frequently employed connection approach in engineering, bolt connections are often subjected to alternating loads caused by factors such as vibration. Under alternating cyclic loads, bolts are highly susceptible to fatigue failure [10–12]. Employing the finite-element method to analyze the stress state of bolts under alternating loads and conducting predictions on the fatigue life of bolts based on the stress state constitutes an effective approach for analyzing the reliability of bolts during their service [13–15]. Yu proposed a new low-cycle fatigue model based on the Von Mises equivalent stress/strain criterion, and then based on the fatigue model and the simulated stress results of the bolt, the fatigue life of the pre-tightened bolt under a high-temperature environment was precisely predicted [16]. Fatigue life prediction further plays a crucial role in optimizing the connection structure. Mrówczyński et al. simulated the stress conditions of two different bolted connection structures (i.e., bolts with hexagonal nuts and self-tapping nutless bolts) for photovoltaic panels. They predicted the fatigue life based on the stress variations of the two types of bolts and found that the self-tapping nutless bolt connection structure, which is faster and easier to install, exhibits a similar fatigue performance to the traditional bolt connection structure with hexagonal nuts [17]. Okorn et al. conducted a simulation study to investigate the stress changes of pre-tightened bolts in flange joints under cyclic loading conditions with different sized gaskets, and it was shown that a higher washer reduces the additional stress in the bolt, which further significantly increases the fatigue life of the bolt in the flange joints [18].

The fatigue failure of the bolts at the outlet of the fracturing pump, which are exposed to alternating loads induced by both the vibration of the fracturing pump and the fluid flow in the manifold during operation, necessitates further investigation. In addition, to prevent the fatigue fracture of bolts during operation, it is essential to accurately predict their fatigue life and replace them with new bolts within the fatigue life cycle. Therefore, this paper establishes a finite-element simulation model of the bolt connection structure at the outlet of the fracturing pump using the Abaqus2023 program and conducts dynamic

analysis of the bolt connection structure under different working conditions based on the measured vibration data of the bolt connection flange at the outlet of the fracturing pump. After acquiring the corresponding stress time-history data, the fatigue life analysis of the bolt connection at the outlet of the fracturing pump was conducted using Fe-safe2023 software. The fatigue life analysis aimed to investigate the influence of fracturing operation conditions on the fatigue life of the bolt connection. This research will provide an effective basis for scientific analysis of the stress state of the bolt at the fracturing pump outlet and estimation of the fatigue life of the bolt, which has great significance for ensuring the safe operation of fracturing operations.

2. Materials and Methods

2.1. Dynamic Analysis Model for Stress State Investigation

The stress state of the structure constitutes a key factor influencing its fatigue life. Consequently, the primary step is to construct a dynamic analysis model of the bolt connection structure at the outlet of the fracturing pump by means of Abaqus2023 software for analyzing the stress state of the bolts during service.

2.1.1. Modelling

Figure 1 shows the fracturing pump equipment in the work site. The wireframe annotation area is the bolt connection structure at the fracturing pump outlet. The dynamic analysis model of the bolt connection structure for stress state investigation is established in accordance with the actual dimensions. Figure 2a presents the disassembly diagram of the established bolt connection structure of the fracturing pump outlet. To enhance the calculation efficiency, the model is established based on one-eighth of the bolt connection structure of the fracturing pump outlet, and the specific dimensions of the connection structure are illustrated in Figure 2b. As depicted in the figure, the connection structure primarily comprises a bolt, nut, gasket, flange, and the housing of the fracturing pump. There are two types of bolts used in the bolt connection structure of the fracturing pump outlet. One type is a full-thread bolt, while the other is a double-headed bolt. In this paper, we will also analyze the influence of the bolt type on the stress state and the fatigue life. The two types of bolts share identical dimensions, with a nominal diameter of 25.4 mm and a thread pitch of 3.175 mm. Currently, to improve computational efficiency, the models for bolt stress investigation usually ignore the thread structure on the bolt [17,19]. However, to ascertain the locations where bolt connections might undergo fatigue failure, it is essential to compute the stress distribution at the threaded area with the highest possible accuracy. Therefore, in this paper, as shown in Figure 2, the threads of the bolts are also established through a parametric modeling method [20].

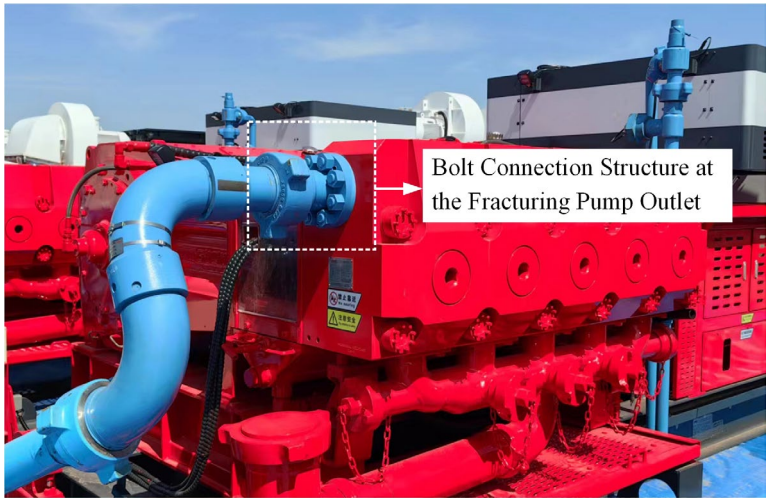


Figure 1. The bolt connection structure at the outlet of the fracturing pump.

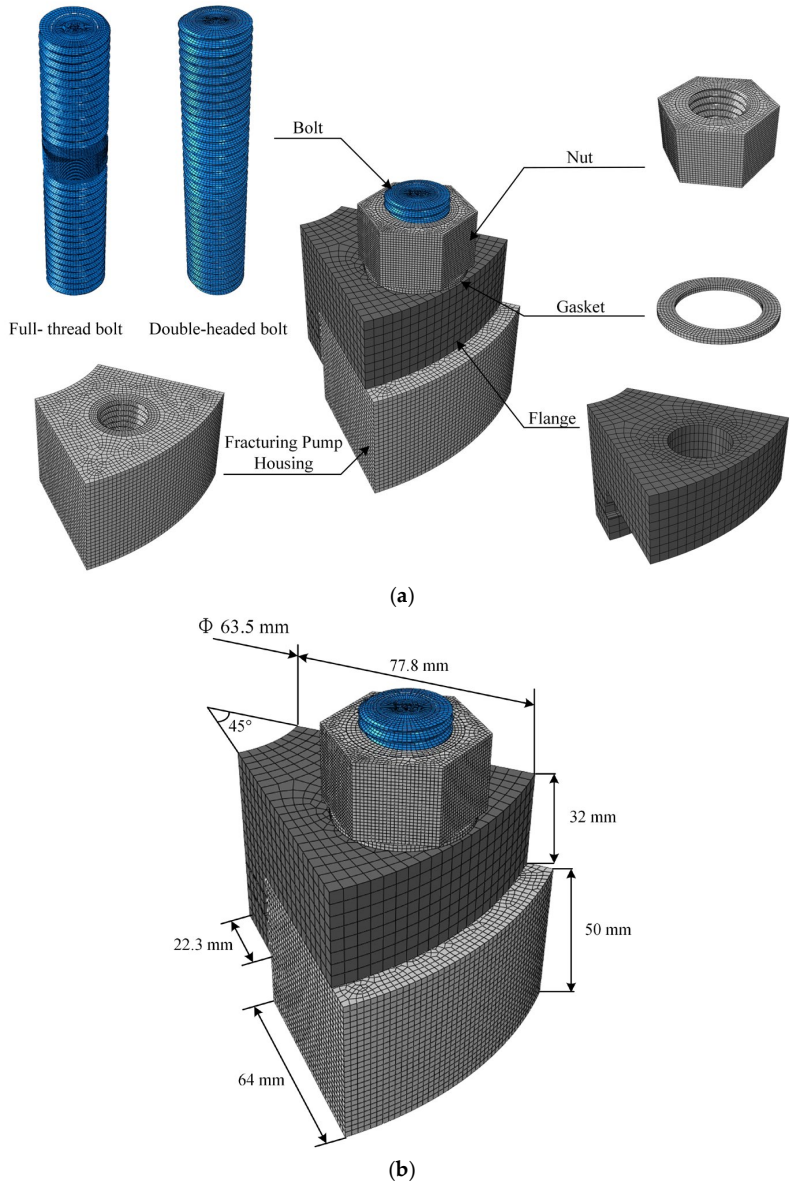


Figure 2. Model of the bolt connection structure at the outlet of the fracturing pump. (**a**) Disassembly diagram of the established bolt connection structure; (**b**) specific dimensions of the connection structure.

2.1.2. Definition for the Element Type and Contact Properties

In the finite-element model of the bolt connection structure at the outlet of the fracturing pump, the bolts and connecting parts are defined as elastic—plastic materials. Both types of bolts were manufactured from the same material, and the mechanical properties of this material were evaluated through laboratory tests. The measured tensile strength is 1260 MPa, the elastic modulus is 211.15 GPa, Poisson's ratio is 0.29, and the yield strength is 1148.77 MPa. The bolt material density is 7850 kg/m^3. The model is meshed by the C3D8R element type, and the total number of model elements is 262,294, while the total number of nodes is 320,041.

Figure 3a presents the sectional schematic diagram of the bolt connection structure. Among them, the contact between the bolt and the nut (as depicted in Figure 3b), as well as the contact between the bolt and the fracturing pump housing (as shown in Figure 3d), are both threaded pairs. The flange has through-hole structures, and the threads of the bolt do not come into contact with the hole walls (as illustrated in Figure 3c). Based on the contact forms among the various components in the model, the contact types in the model are configured. Firstly, the contact of the threaded pair between the bolt and the nut is set as face-to-face contact. In this study, the normal contact employs the "soft contact" method with the contact algorithm set to the "exponential method", whereas the tangential contact utilizes the penalty function contact algorithm. For the threaded contact between the bolt and the fracturing pump housing, as well as the contact between other components in the model, a general contact type is used for setting. Additionally, there will be small relative sliding between the contact surfaces, so all contacts are calculated using the finite sliding formula, with a tangential direction using a penalty function contact algorithm, and with a friction coefficient of 0.15, except for the threaded contact between the bolt and nut, where the normal contact of the other contact surfaces is constrained by "hard contact".

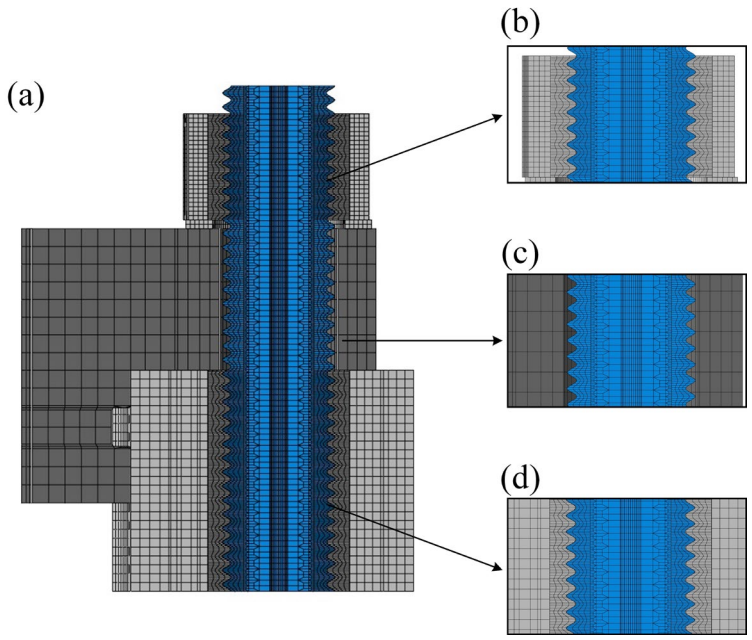


Figure 3. Contact of the bolt connection structure at the outlet of the fracturing pump. (**a**) Cross-section of bolt connection structure; (**b**) threaded pair between the bolt and the nut; (**c**) bolt holes through flange; (**d**) threaded pair between fracturing pump housing and bolt.

2.1.3. Analysis Step

As shown in Figure 4, the stress simulation of the bolt connection structure at the fracturing pump outlet includes three analysis steps:

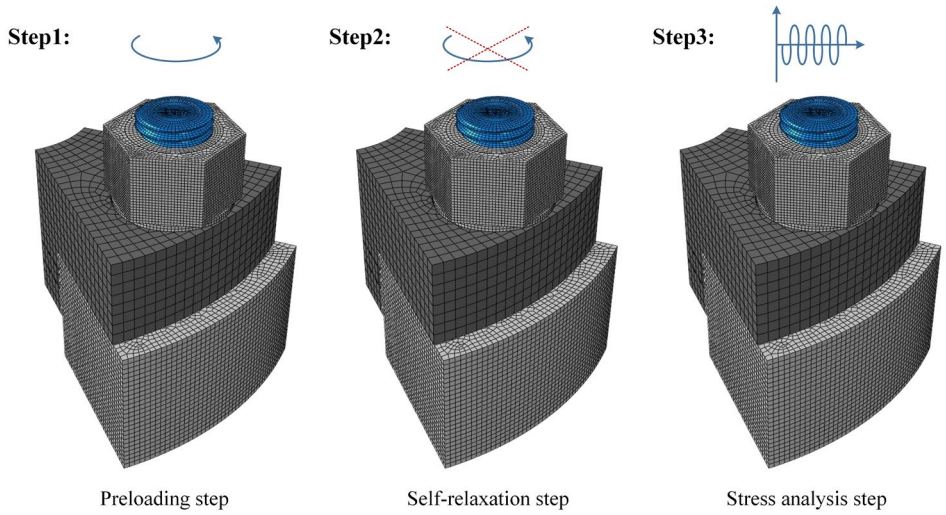


Figure 4. Analysis step for stress simulation of the bolt connection structure.

(1) Step 1: Analysis Step 1 is the preload application analysis step, with a duration of 1 s. This analytical step is utilized to simulate the pre-tensioning process of the bolt connection under the application of tightening torque.

(2) Step 2: Analysis Step 2 is the self-relaxation analysis step of the bolts, with a duration of 1 s. This analysis procedure is adopted to simulate the self-relaxation stage of the bolt connection subsequent to the release of the tightening torque.

(3) Step 3: Analysis Step 3 is the analysis step for applying vibrational displacement loads to the bolts at the outlet of the fracturing pump, with a duration of 2 s. This analysis step will simulate the stress state of the bolts at the outlet of the fracturing pump under the action of vibrational displacement loads.

2.1.4. Constraints and Load Applications

Based on the aforementioned simulation targets of the three analysis steps, the constraints and loads of each analysis step are configured.

(1) Step 1: To simulate the preloading state of the bolt more accurately, in this paper, the tightening process of the nut is simulated by applying angular load to the nut, thereby achieving the pretension of the bolt. Figure 5 presents the schematic diagram for the application of angular load on the nut. By means of kinematic coupling, the outer surface of the nut is coupled with the reference point Nut_RP, and subsequently, the angular load is applied to the reference point Nut_RP, with a rotation angle of 0.48 rad. Through the preliminary test simulation, it was found that the equivalent tightening torque for the nut under this angle was 960 N·m, which met the required torque for actual engineering applications. Additionally, the remaining components in the model must be constrained with necessary constraints. The gaskets, flanges, and housing are all constrained in the x and z directions, retaining y-direction freedom, to ensure that the components can undergo coordinated axial deformation under the preload force of the bolts during the nut tightening process.

(2) Step 2: In this analysis step, the rotational load of the nut will be revoked, and the flange constraint will be released. Only the original constraints of the gasket and the fracturing pump housing will be retained. This process mimics the actual operation where, after the tightening torque is removed, the pretension load of the bolts drops due to factors such as torsional deformation, resulting in a self-relaxation process.

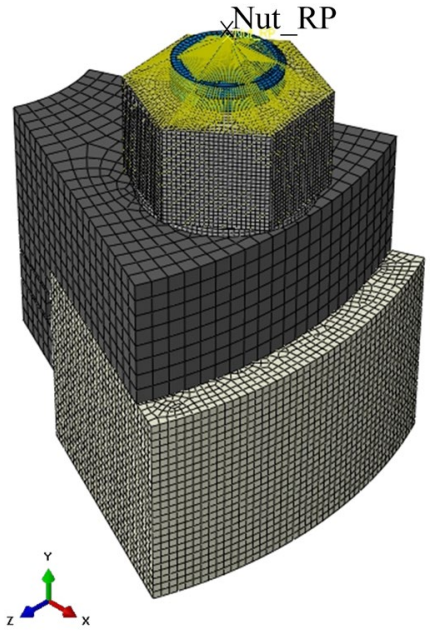
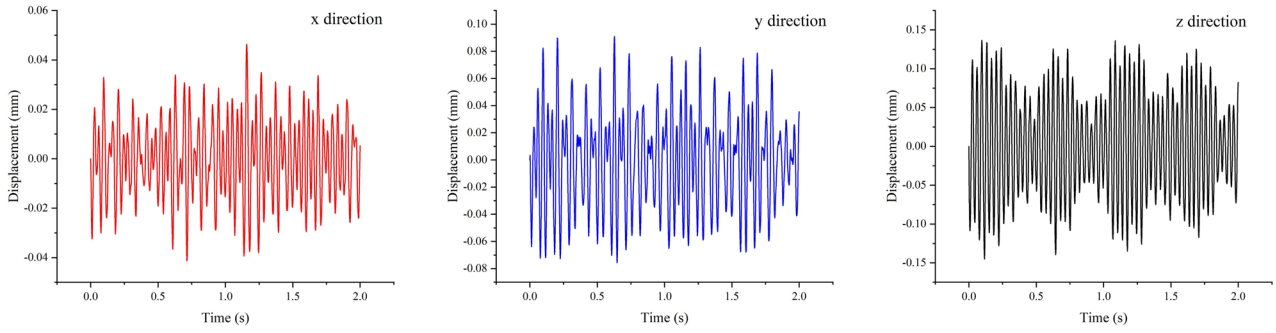


Figure 5. Rotational load applied to the nut.

(3) Step 3: Once the self-relaxation stage is accomplished, the vibrational displacement loads is exerted on the fracturing pump to acquire the stress state of the bolt connection structure at the pump outlet. In engineering applications, the driving methods of fracturing pumps mainly consist of three types, including the diesel-driven method, single-motor-driven method, and dual-motor-driven method. In this paper, the displacement data of the bolt connection structure at the outlet end of the fracturing pump under the three driving methods were collected on-site, which are depicted in Figure 6. The application of displacement load is also carried out by means of kinematic coupling. As illustrated in Figure 7, three reference points, namely X_RP, Y_RP, and Z_RP, are established in the model. Y_RP is coupled to the upper surface of the fracturing pump housing, while X_RP and Z_RP are coupled to the side of the fracturing pump housing. A displacement load in the y-direction is imposed on Y_RP, and displacement loads in the x and z-directions are applied to X_RP and Z_RP, respectively.



(**a**)

Figure 6. *Cont.*

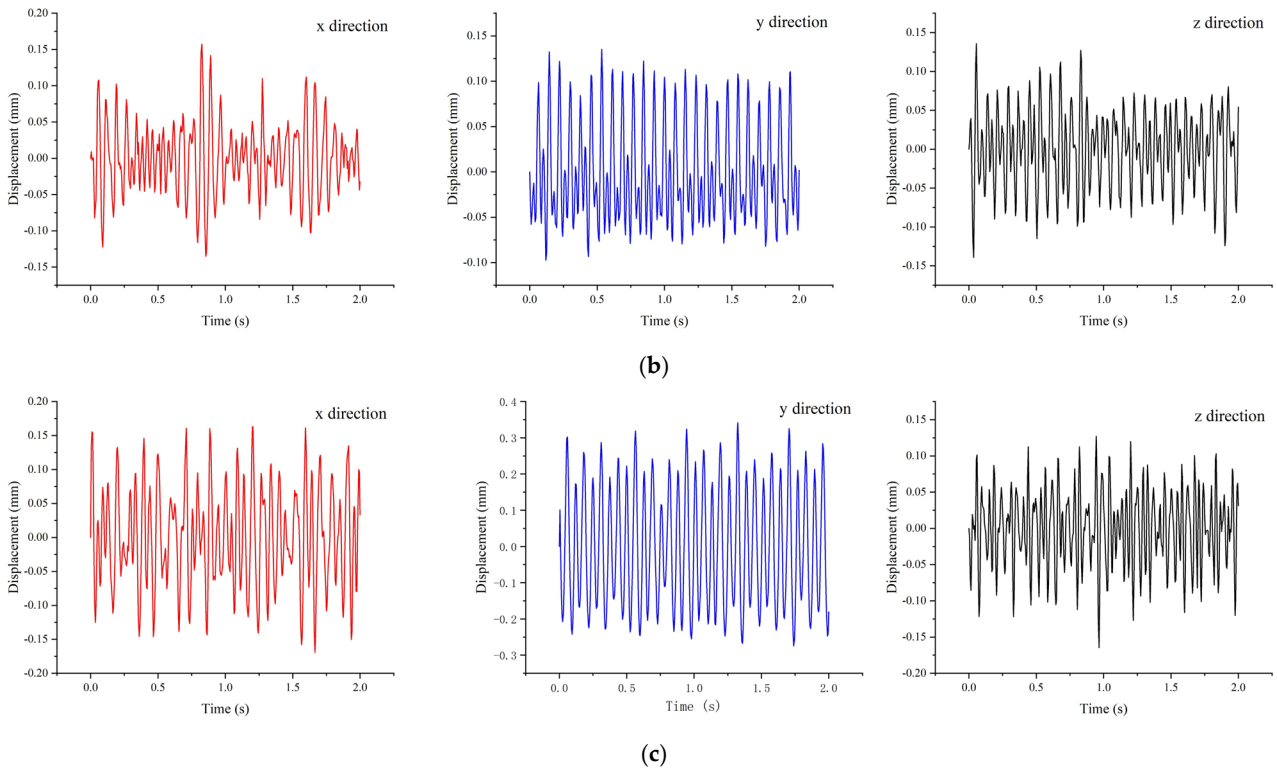


Figure 6. Displacement data of the bolt connection structure under different driving methods. (**a**) Diesel-driven method; (**b**) single-motor-driven method; (**c**) dual-motor-driven method.

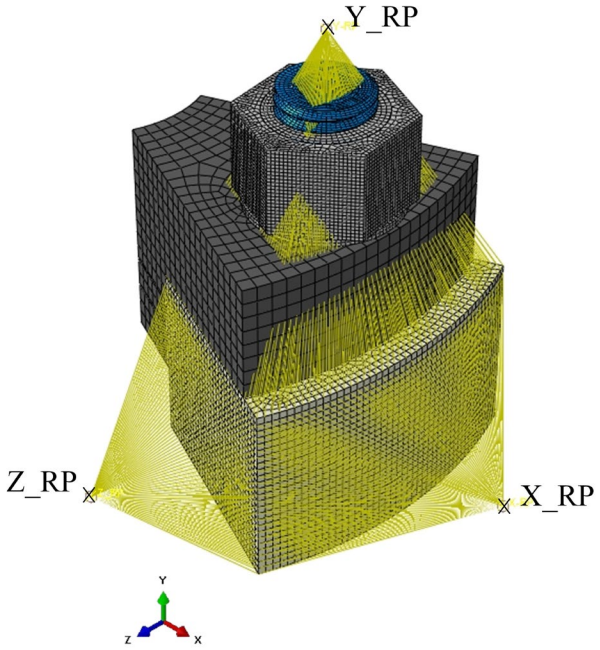


Figure 7. The application of displacement load for the bolt connection structure.

2.2. Fatigue Hypotheses

Based on the vibrational displacement load and structural characteristics of the bolt, it can be concluded that the bolt experiences multi-axial stress internally. The critical plane method is widely recognized as an effective multi-axial fatigue failure criterion [21,22]. The determination of the critical plane is influenced by damage parameters; therefore, the choice of damage criterion significantly affects the accurate prediction of fatigue life. According to the Brown—Miller fatigue hypothesis, fatigue cracks initially nucleate along

the maximum shear plane and subsequently propagate perpendicular to the direction of maximum tensile strain [23,24]. This criterion offers a comprehensive explanation of crack initiation and propagation at the microscopic level, possesses significant physical meaning, and is widely acknowledged by researchers as an effective method for analyzing multi-axial fatigue. Therefore, this paper employs the Brown—Miller fatigue hypothesis based on the critical plane criterion to simulate and calculate the fatigue life of the bolt at the outlet of the fracturing pump, which takes the following form [25]:

$$\frac{\Delta\gamma_{max}}{2} + \frac{\Delta\varepsilon_n}{2} = 1.65\frac{\sigma'_f}{E}\left(2N_f\right)^b + 1.75\varepsilon'_f\left(2N_f\right)^c \quad (1)$$

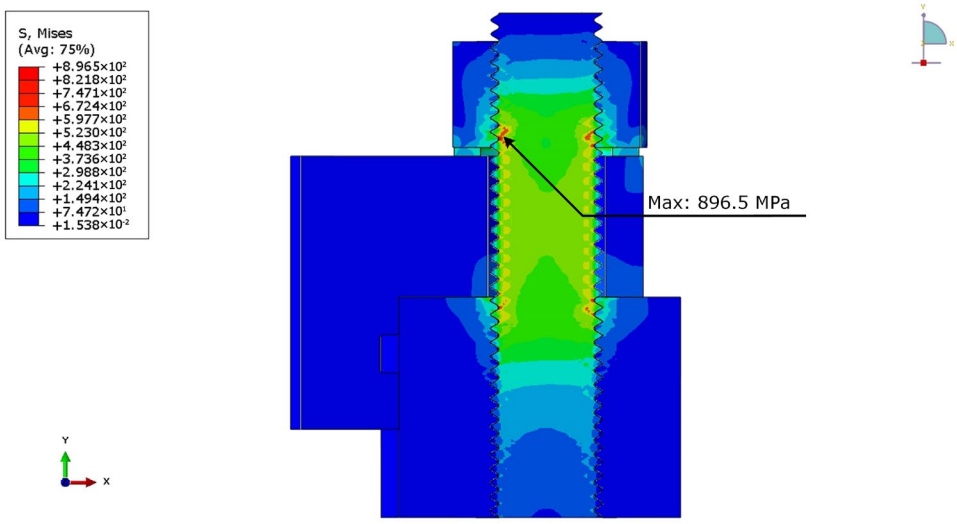
where γ_{max} is the maximum shear strain, ε_n the normal strain in the maximum shear strain plane, σ'_f the fatigue strength coefficient, E the elasticity modulus, N_f the fatigue life, and ε'_f the fatigue ductility coefficient.

The stress results obtained from the dynamic analysis of two types of bolts under different load conditions were imported into Fe-Safe for fatigue life analysis. The number of fatigue cycles at each node of the bolts was statistically counted using the Rainflow counting method, thereby obtaining the fatigue life of the bolts [26,27].

3. Results and Discussions

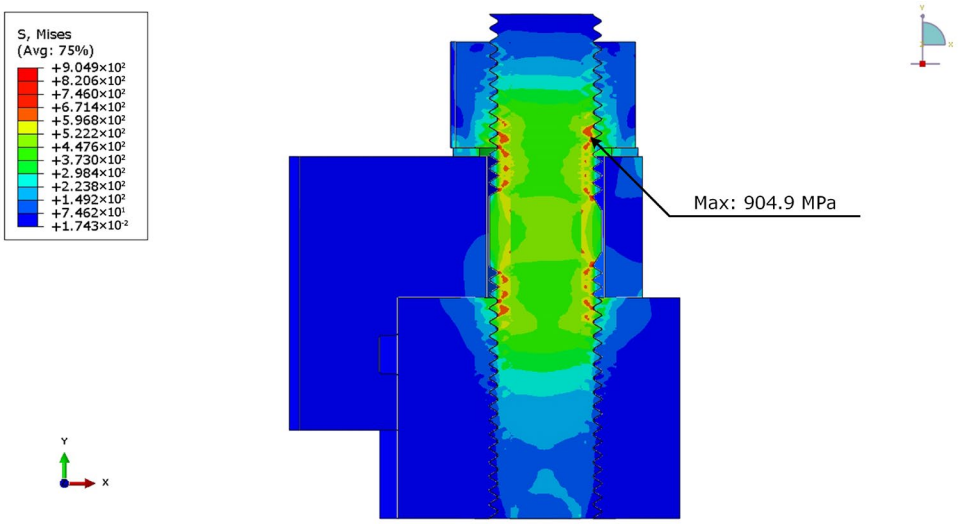
3.1. Stress State of the Bolt at the Outlet End of the Fracturing Pump

Figure 8 shows the stress distribution of two types of bolts after preload and self-relaxation is complete. The maximum stress values of the full-thread bolt and double-headed bolt after self-relaxation is complete are 896.5 MPa and 904.9 MPa, respectively. It is found that, under the same tightening torque, the maximum stress value of the double-headed bolt is slightly higher than that of the full-thread bolt. In addition, the maximum stress values of the full-thread bolt and double-headed bolt in this stage are both approximately 78% of the yield stress, which meet the requirement of the DASt-Guideline 021 German standard [28].



(**a**)

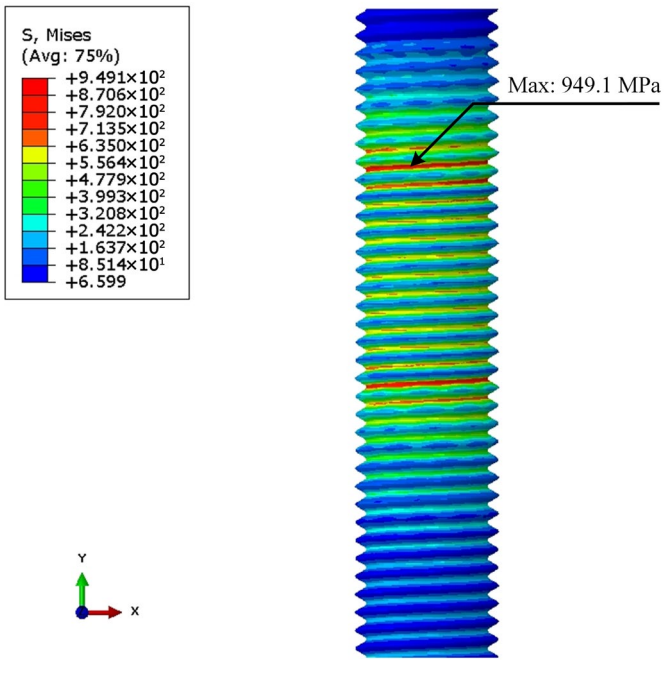
Figure 8. *Cont.*



(**b**)

Figure 8. The stress distribution of two types of bolts after preload and self-relaxation. (**a**) Full-thread bolt; (**b**) double-headed bolt.

Figure 9a–c, respectively, present the stress distribution of the full-thread bolt under the three different types of displacement loads when the loading time is 1 s. Under the effect of displacement load, stress concentration emerges at the thread corresponding to the contact surface between the nut and the gasket and at the thread corresponding to the contact surface between the flange and the housing. The stress concentration region is frequently the location where bolts initially experience fatigue fracture. Among them, the maximum stress value occurs at the thread corresponding to the contact surface between the nut and the gasket.



(**a**)

Figure 9. *Cont.*

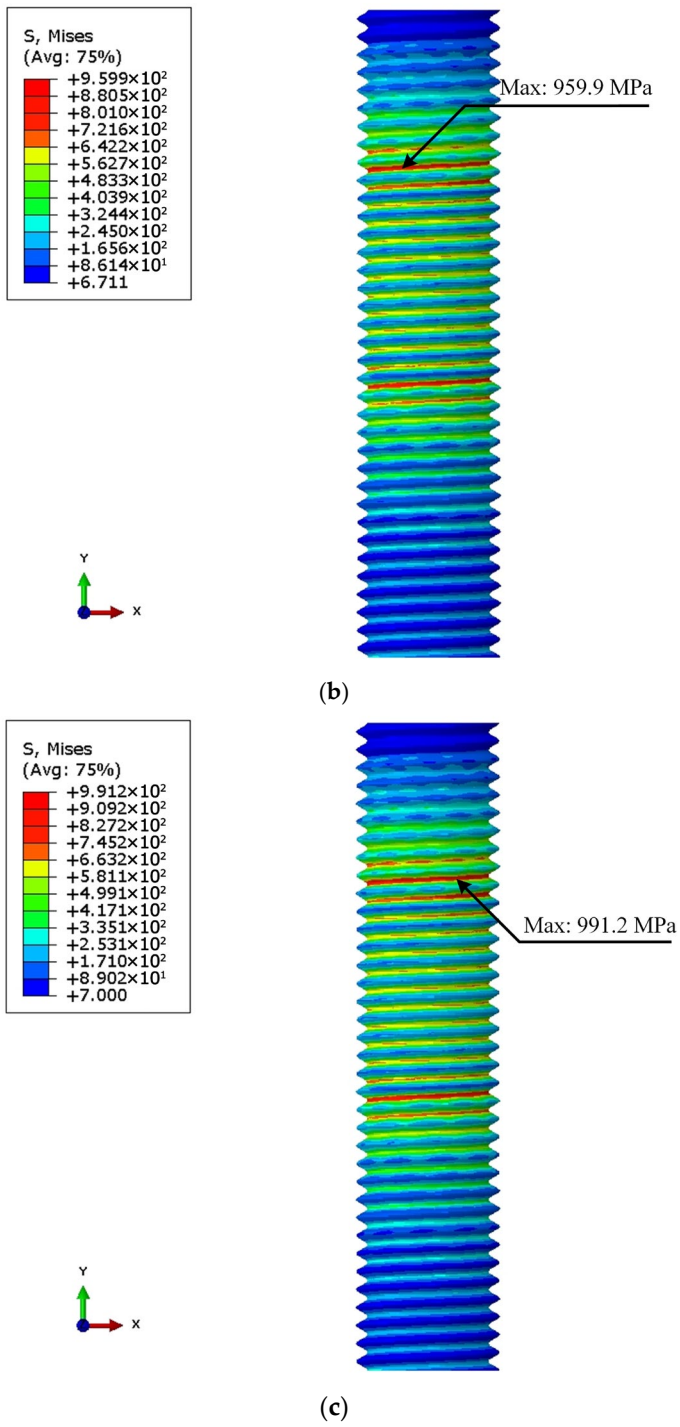


Figure 9. The stress distribution of full-thread bolt under different types of displacement loads. (**a**) Diesel-driven method; (**b**) single-motor-driven method; (**c**) dual-motor-driven method.

Figure 10 shows the time history of maximum stress for full-thread bolts under three types of load. The maximum stress and the amplitude of stress variation of the full-thread bolt under the displacement load of the dual-motor-driven method are 1076.3 MPa and 234.8 MPa, which are conspicuously higher than those when subjected to the displacement load of single-motor-driven and diesel-driven methods. Among the three driving methods, the maximum stress level and the amplitude of stress variation for the full-thread bolts subjected to displacement loads using the diesel-driven method are the lowest. The maximum and minimum stress values in this case are 957.8 MPa and 905.9 MPa, respectively. The difference in stress is primarily attributed to the variations in displacement load under

different driving methods. According to the displacement data shown in Figure 6, it is noted that under the dual-motor-driven method, the vibration displacement amplitude of the bolt connection structure reaches the maximum. Among them, the vibration amplitude in the y direction is significantly higher than that in the x and z directions. The maximum amplitude in the y direction is approximately 0.621 mm, and the maximum vibration amplitudes in the x and z directions are 0.344 mm and 0.308 mm, respectively, while under the diesel-driven method, the maximum vibration amplitude emerges in the z direction, approximately 0.291 mm, and it is significantly less than the vibration amplitudes in all directions under the dual-motor-driven method. The primary distinctions among the displacements for the three driving methods of fracturing pump lie in the providers and forms of their power sources. In the diesel-driven method, the fracturing pump utilizes diesel as the power source. The mechanical power generated by the combustion process in the diesel engine drives the pump to operate. Both the single-motor-driven method and the dual-motor-driven method employ motor-driven systems. The key distinction is that the single-motor-driven utilizes a single motor for propulsion, whereas the dual-motor-driven method employs two independently operated motors.

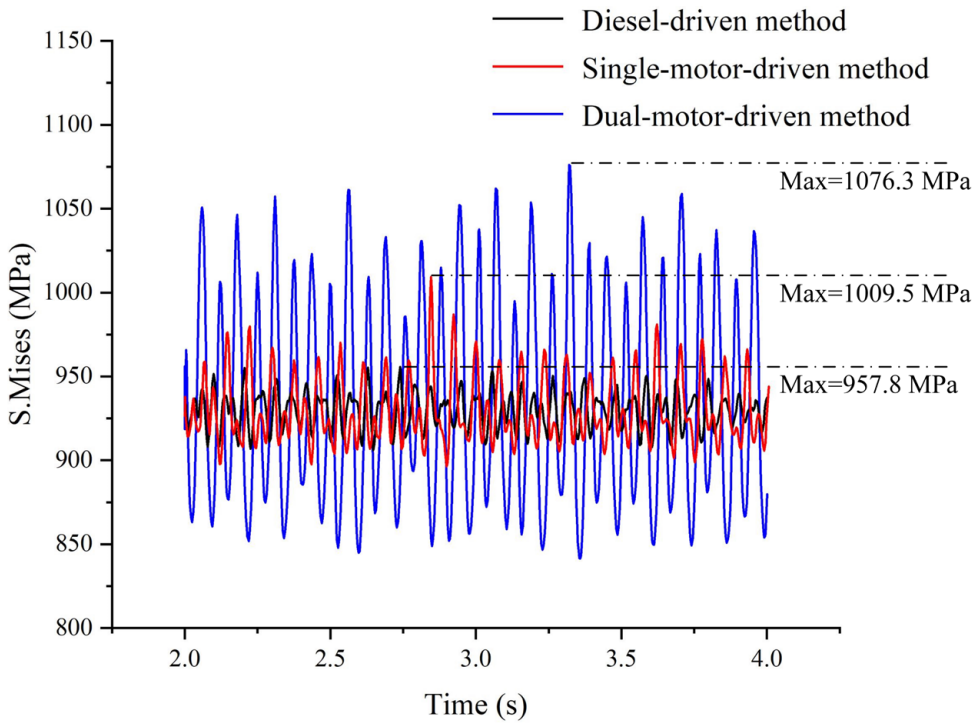
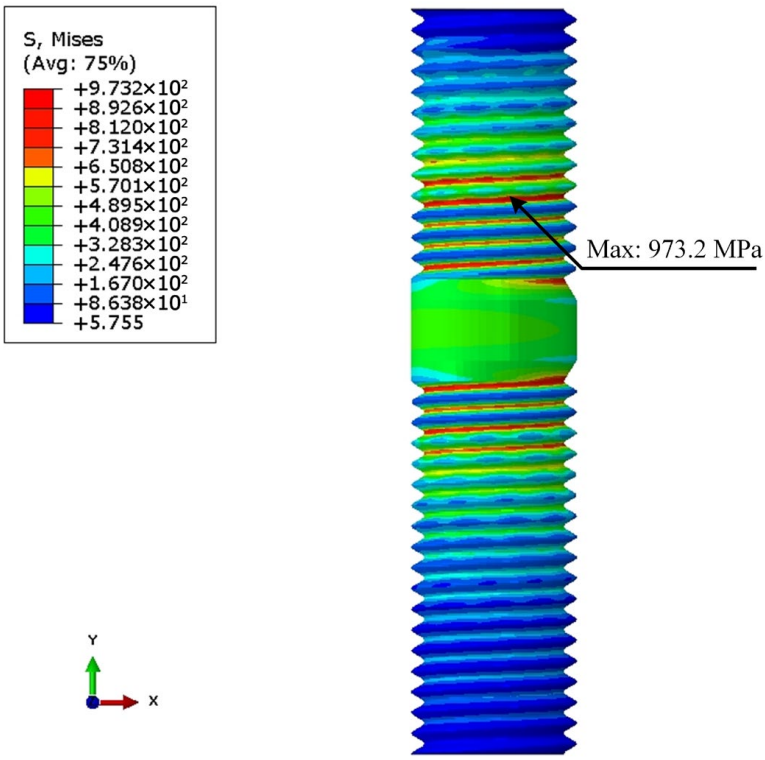
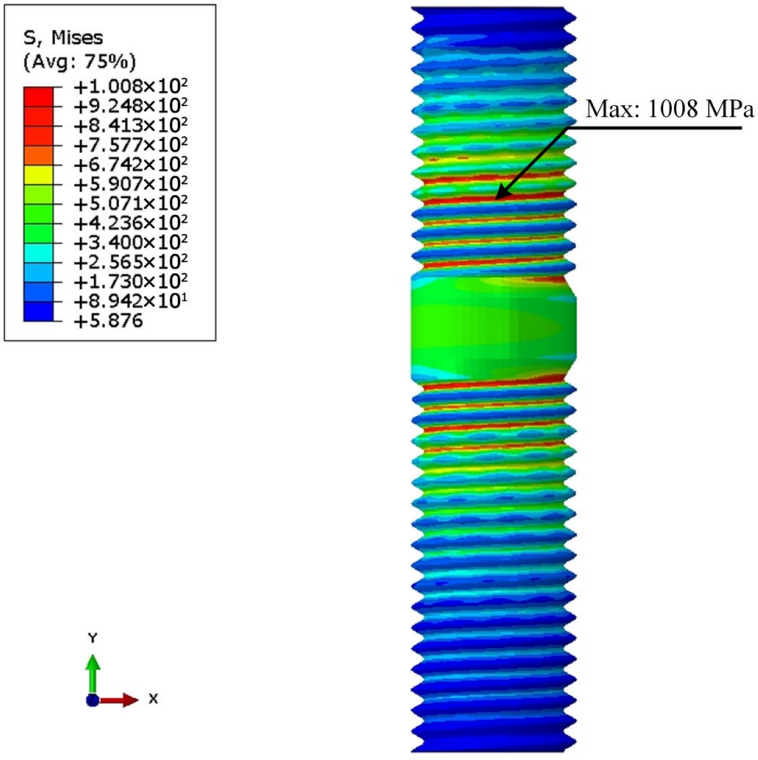


Figure 10. Time history of maximum stress for full-thread bolt under three types of load.

Figure 11 depicts the stress distribution within the double-headed bolt after 1 s of vibration loading under three different driving methods. By analyzing the stress concentration regions of the bolts in this structure, it can be observed that apart from the threaded area corresponding to the contact surface of the nut and the gasket, stress concentration also emerges in the transition zone between the rod and the threads section. Nevertheless, the maximum stress of the double-headed bolt still lies in the threaded area corresponding to the contact surface of the nut and the gasket.

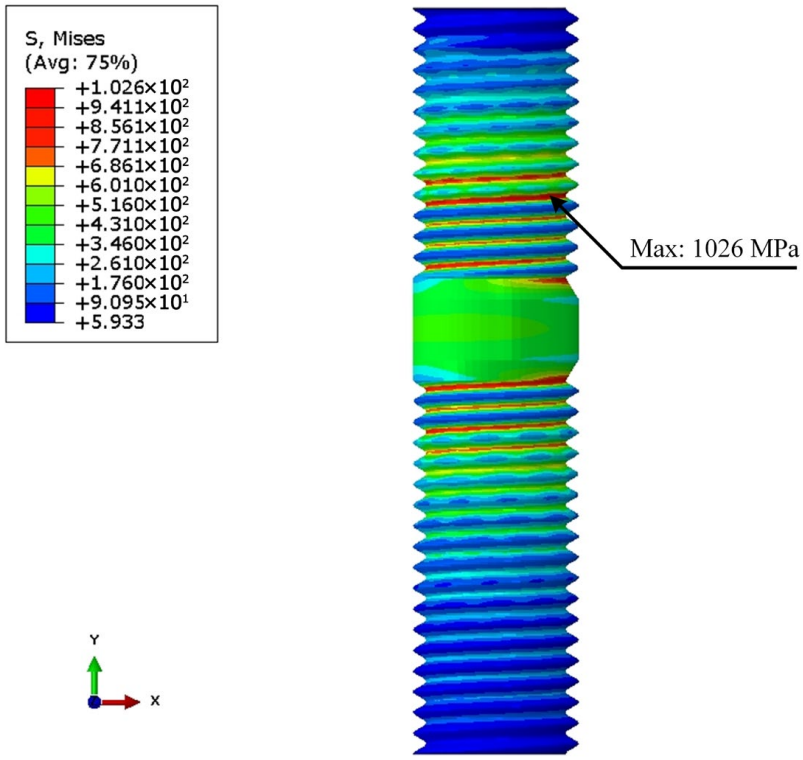


(**a**)



(**b**)

Figure 11. *Cont.*



(**c**)

Figure 11. The stress distribution of double-headed bolt under different types of displacement loads. (**a**) Diesel-driven method; (**b**) single-motor-driven method; (**c**) dual-motor-driven method.

The maximum stress of the double-headed bolt under three different types of displacement loads was extracted, as shown in Figure 12. Due to the relatively larger vibration displacement amplitude, the maximum stress and stress variation amplitude under the displacement load of the dual-motor-driven method were higher than those of the other two types of loading. To explicitly determine the impact of bolt types on their internal stress states, the stress variation curve of two types of bolts under the same type of load was compared. Figure 13a–c show the time-history curves of stress for the two types of bolts under different types of displacement loads. It can be seen that under the displacement load of the dual-motor-driven method, the stress variation amplitude of the double-headed bolt is the largest, reaching 396 MPa, which is 161.2 MPa greater than that of the full-thread bolt under the same load. Under the displacement load of the diesel-driven method, the stress variation amplitude of the full-thread bolt is observed to be the smallest, at 51.9 MPa. Under the same loading condition, the stress variation range of the double-headed bolt increases slightly to 87.4 MPa. It should be noted that under the displacement load of the single-motor-driven method, the difference in stress variation amplitude between the two types of bolts is relatively minor. From the viewpoint of the two bolt structures, this is primarily attributed to the fact that the full-thread bolt has a greater number of threads compared to the double-headed bolt. That is, there are more thread root areas available for sharing the internal stress, thereby reducing the concentrated stress level formed at the thread roots. From this viewpoint, the full-thread bolt is superior to the double-headed bolt featuring a smooth shank. Specifically, the stress variation amplitude of the double-headed bolt increases by only 16 MPa compared to that of the full-thread bolt. This indicates that under the displacement load of single-motor-driven method, the stress variation amplitude of the bolts is relatively insensitive to the bolt type.

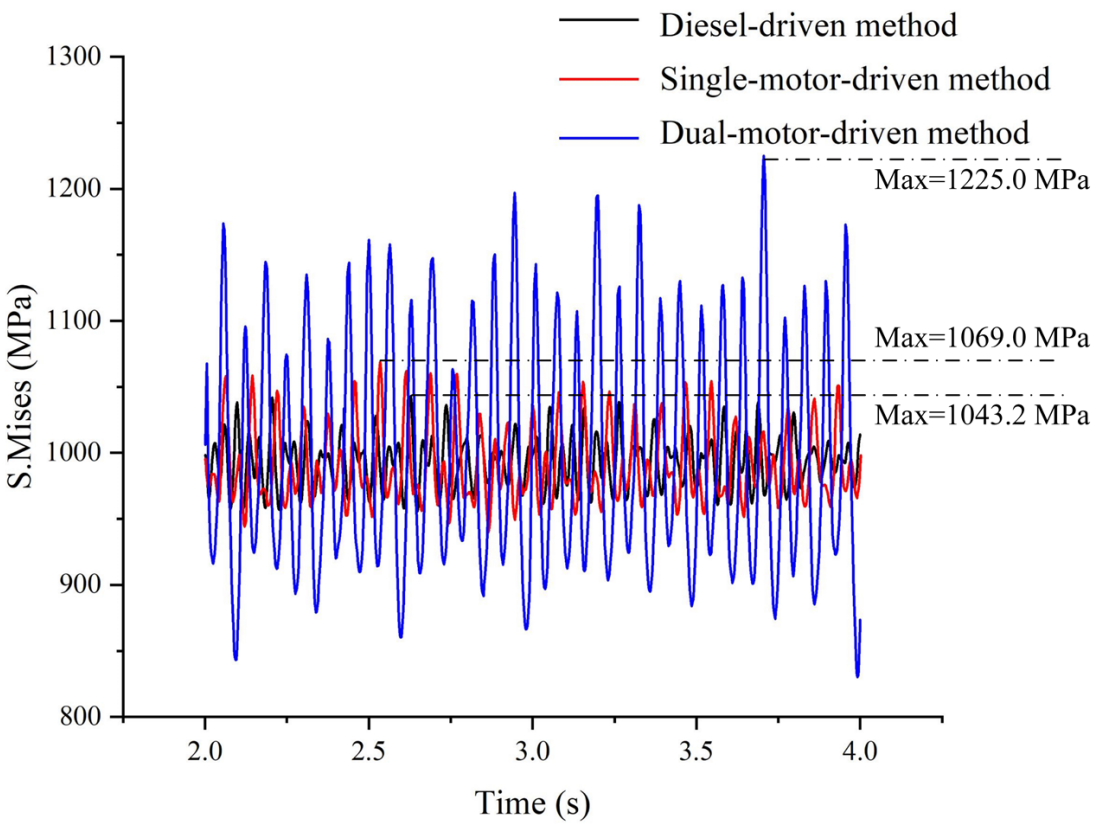


Figure 12. Time history of maximum stress for double-headed bolt under three types of load.

3.2. Fatigue Life of the Bolt at the Outlet End of Fracturing Pump

It can be seen from the stress analysis of the fracturing pump outlet bolt that the bolt undergoes a non-stable variable stress process under the action of multi-axis vibration load. Under the sustained influence of this non-stable variable stress, the bolt is prone to undergo fatigue fracture failure. The stress results obtained from different types of loads in the dynamic analysis of two types of bolts were imported into the Fe-Safe software for fatigue life analysis. The number of fatigue cycles at each node of the bolt was statistically counted using the rain-flow counting method, thereby obtaining the fatigue life of the bolt. Upon the completion of the analysis, the number of stress cycles is transformed into the fatigue life measured in hours. Figure 14 presents the bolt life of the full-thread bolt under three different types of loads, the fatigue life value was present in loglife. It is observable that the earliest position of fatigue failure in the full-thread bolt within this structure is situated at the interface between the nut and the washer, corresponding to the thread root. In accordance with the stress distribution of the full-thread bolt under different types of loads, this location is precisely the area where the maximum stress emerges. Under the individual loadings of the diesel-driven method, single-motor-driven method, and dual-motor-driven method, the fatigue life of the full-thread bolt decreases in the sequence presented in Figure 15, namely 2042.89 h, 1351.05 h, and 1014.24 h. It can be seen from the stress state of the full-thread bolt under the three load conditions that the maximum stress and the amplitude of stress fluctuation are significantly higher under the load condition of the dual-motor-driven method than under the other two load conditions. In this situation, the fatigue damage induced by stress to the full-thread bolt is relatively significant, thereby causing it to fail earliest. Consequently, the fatigue life of the full-thread bolt is shorter in this case.

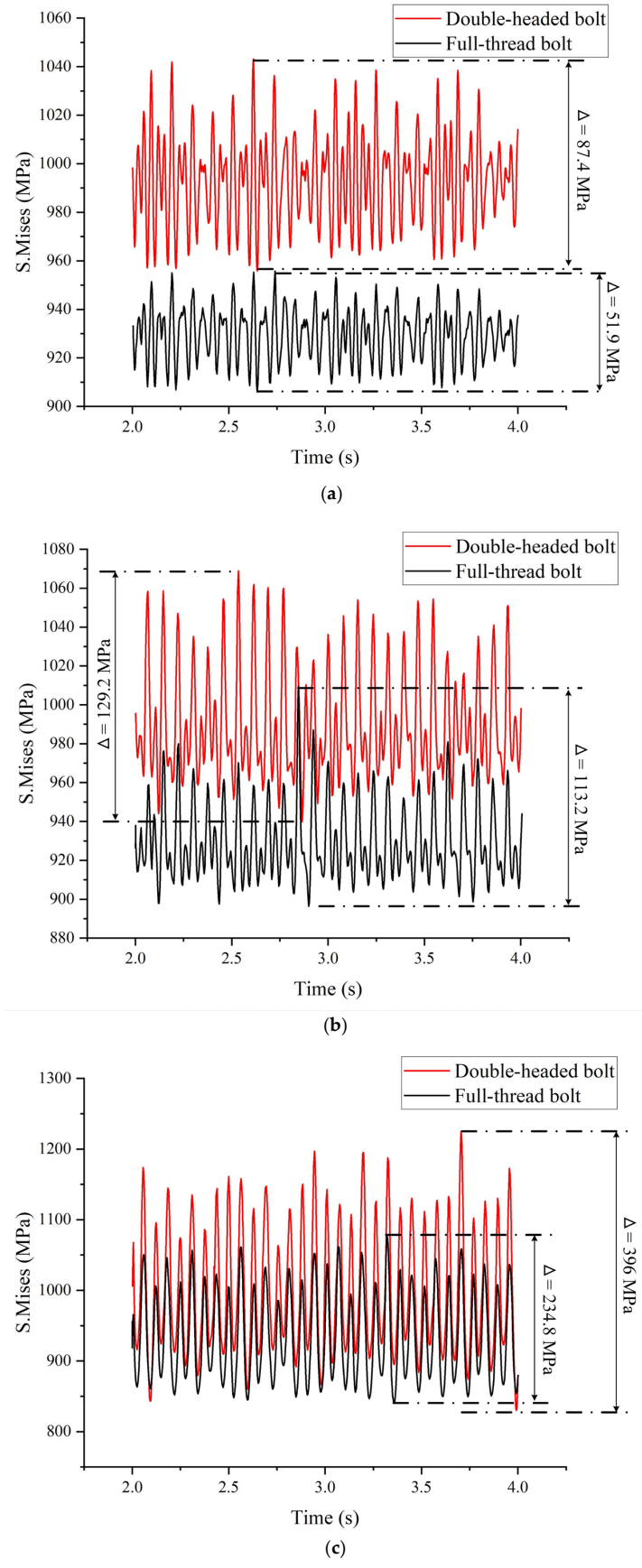
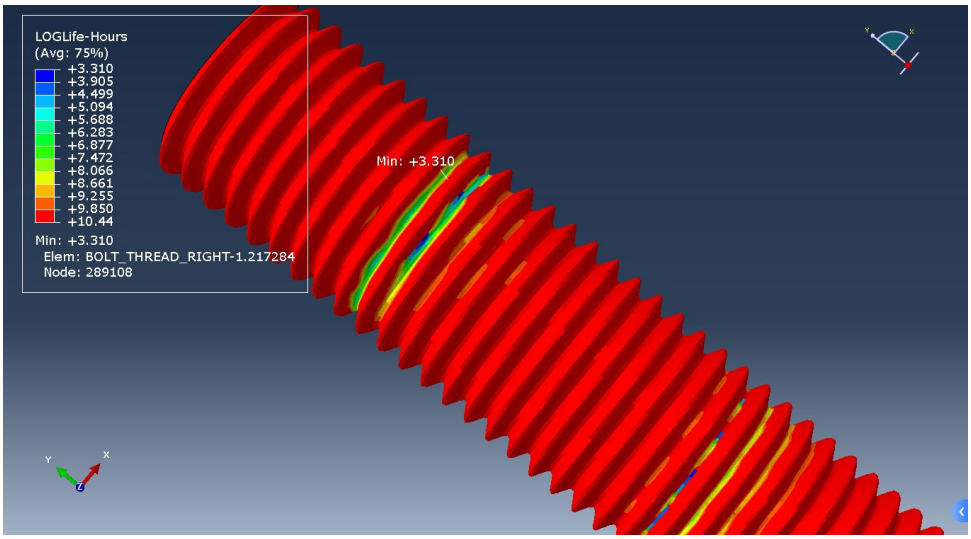
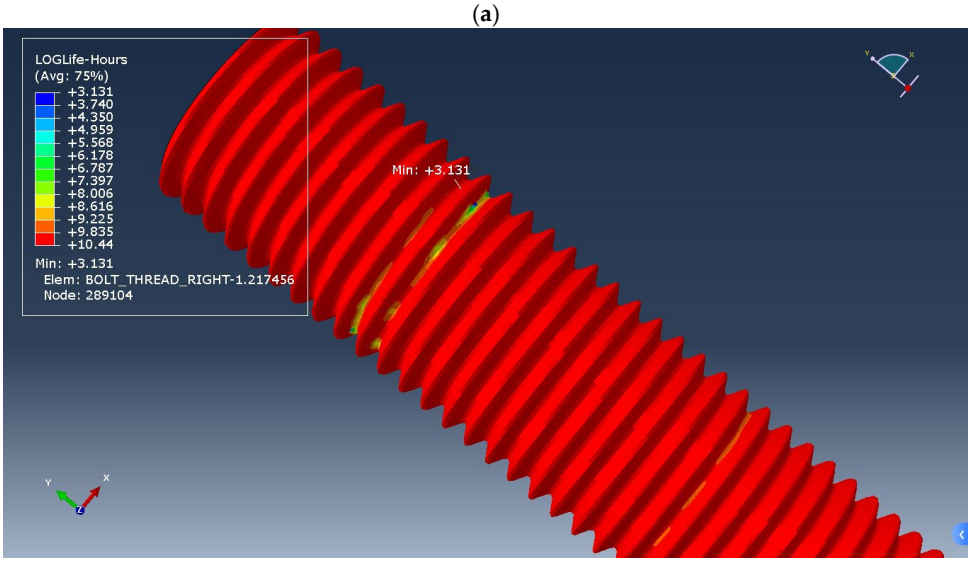


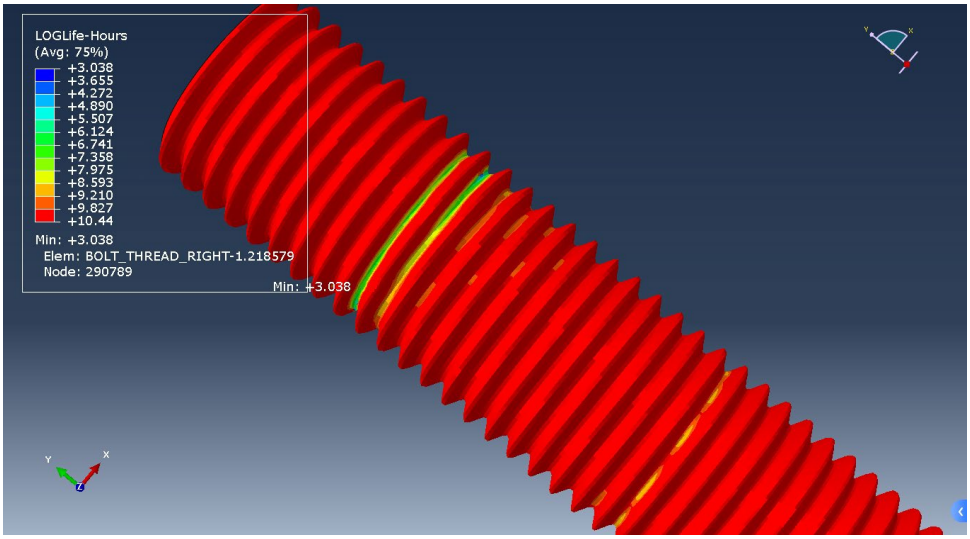
Figure 13. Comparison of maximum stress variation for double-headed bolt and full-thread bolt under three types of load. (**a**) Diesel-driven method; (**b**) single-motor-driven method; (**c**) dual-motor-driven method.



(**a**)



(**b**)



(**c**)

Figure 14. Fatigue life of the full-thread bolt under three different types of loads. (**a**) Diesel-driven method; (**b**) single-motor-driven method; (**c**) dual-motor-driven method.

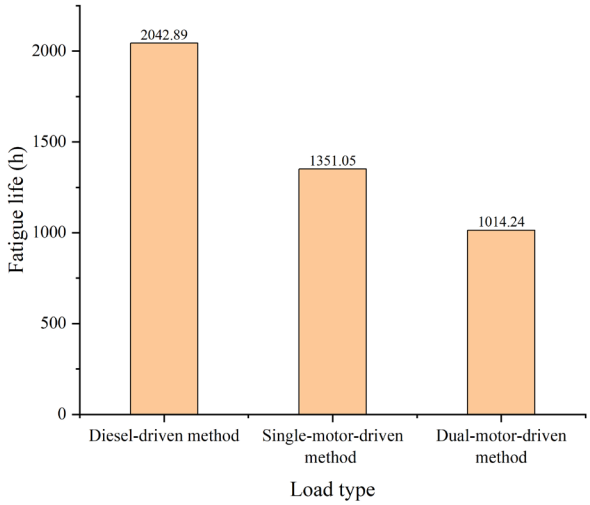


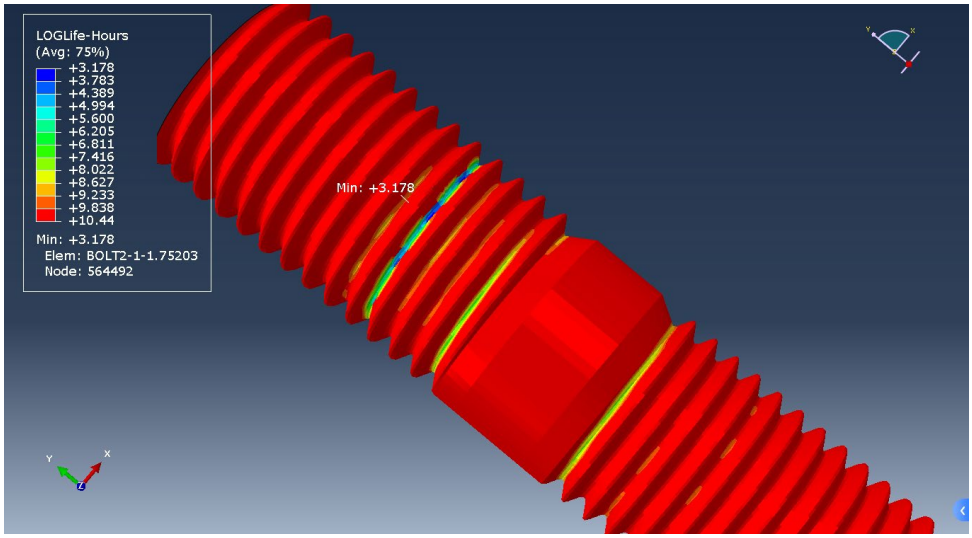
Figure 15. Comparison in fatigue life of full-thread bolt under three different types of loads.

Figure 16 presents the bolt life of the double-headed bolt under different types of loads. When compared with the stress distribution of the double-headed bolt under different vibrational displacement loads in the dynamic analysis, it can be observed that the stress concentration area is the main region of fatigue damage, and the area where fatigue failure occurs is the region where the maximum stress is located. Comparing the fatigue life of the double-headed bolt under three load conditions, it can be seen that in this structure, the fatigue life of the double-headed bolt under the load conditions of diesel-driven, single-motor-driven, and dual-motor-driven method is successively reduced, respectively, as 1505.72 h, 1223.97 h, and 717.46 h. This is primarily attributed to the circumstance that when exposed to the loads of the dual-motor-driven method, the maximum stress and stress variation range of the double-headed bolt within the structure are comparatively large, resulting in substantial fatigue damage to the bolts and thereby lowering the fatigue life.

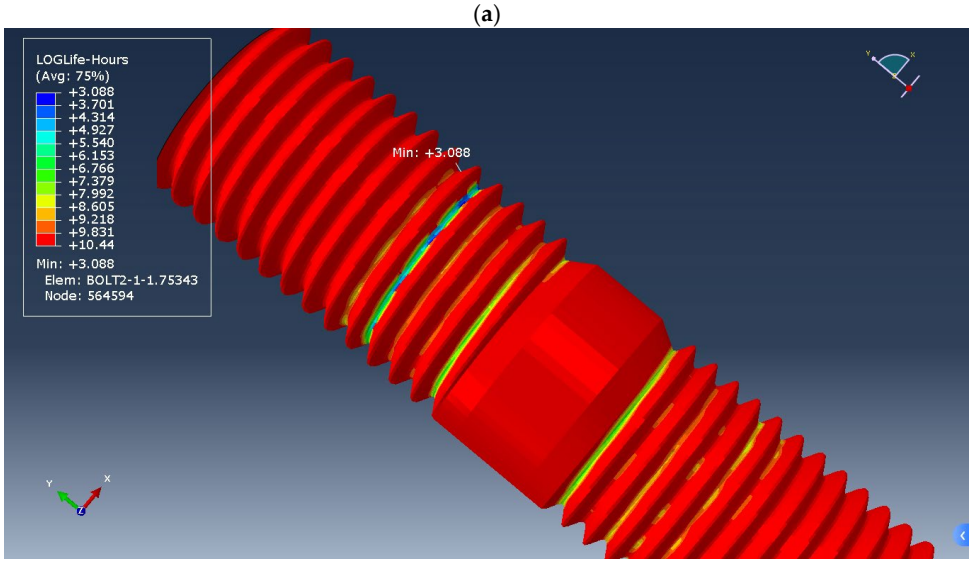
Comparing the fatigue life of the two types of bolts under the same load can further reflect the influence of the bolt type on the fatigue life. As shown in Figure 17, under the same load, the fatigue life of the double-headed bolt is shorter than that of the full-thread bolt. By comparing the stress states of the two types of bolts under the same type of load, it can be seen that the maximum stress and stress variation range of the double-headed bolt are higher than the stress level of the full-thread bolt under the same load. Therefore, the damage to the bolt caused by the double-headed bolt is greater, and its fatigue life is obviously shortened. Table 1 further compares the predicted fatigue life values with the actual field monitoring values in engineering projects. It can be noted that based on the stress state and the fatigue hypotheses, the fatigue life of the bolts at the outlet end of fracturing pump can be well predicted.

Table 1. Comparison of the predicted fatigue life and actual field monitoring life.

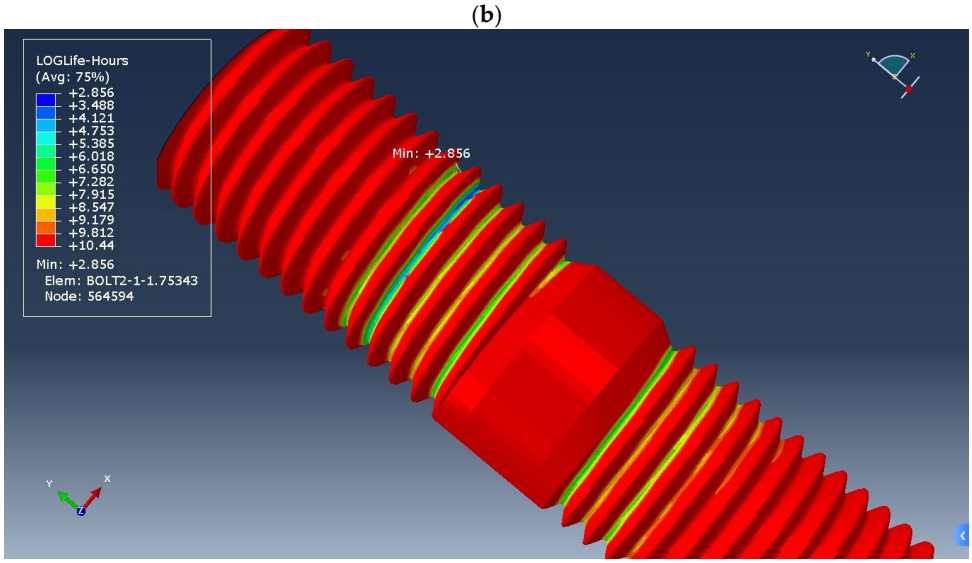
Bolt Type	Vibrational Displacement Condition	Predicted Fatigue Life (h)	Average Actual Field Monitoring Life (h)
Full-thread bolt	Diesel-driven method	2042.89	1735
	Single-motor-driven method	1351.05	1240
	Dual-motor-driven method	1014.24	1159
Double-headed bolt	Diesel-driven method	1505.72	1296
	Single-motor-driven method	1223.97	1034
	Dual-motor-driven method	717.46	605



(**a**)



(**b**)



(**c**)

Figure 16. Fatigue life of the double-headed bolt under three different types of loads. (**a**) Diesel-driven method; (**b**) single-motor-driven method; (**c**) dual-motor-driven method.

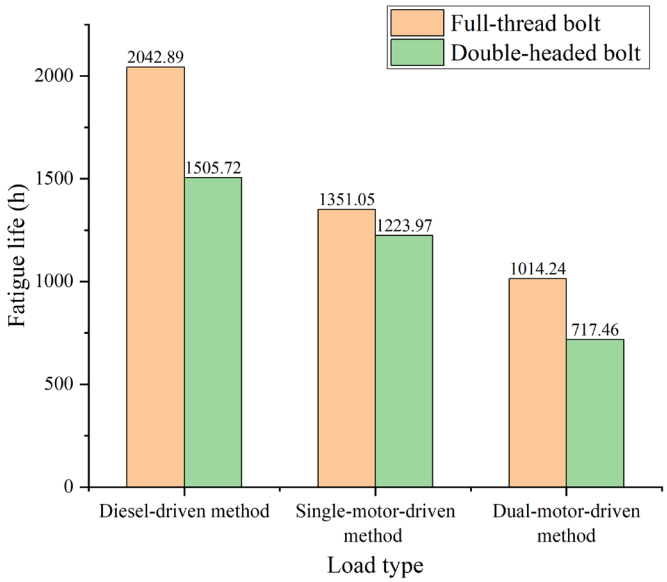


Figure 17. Comparison of fatigue life of two types of bolts under the same loading conditions.

4. Conclusions

In this paper, the stress state of the bolts at the outlet end of the fracturing pump is numerically evaluated, and the influence of bolt type and vibrational displacement loads is investigated. Based on these stress analyses, the fatigue life under various conditions is predicted. The key findings are summarized as follows:

(1) For both the double-headed bolt and the full-thread bolt, the maximum stress and stress variation amplitude increase in the sequence of diesel-driven, single-motor-driven, and dual-motor-driven loadings. This trend is primarily attributed to the greater displacement amplitude experienced under dual-motor-driven conditions.

(2) Under the same load, the maximum stress and stress variation amplitude of the full-thread bolt are significantly lower than those of the double-headed bolt. This is mainly because the full-thread bolt is a full-thread structure; there are more thread root areas available for sharing the internal stress, thereby reducing the concentrated stress level formed at the thread root.

(3) The fatigue life of the two types of bolts decreases in sequence under the three load conditions of the diesel-driven, single-motor-driven, and dual-motor-driven methods, mainly due to the gradual increase in stress level. Due to the lower stress state of the full-thread bolt compared with the same load condition of double-headed bolt, its fatigue life is relatively longer. Therefore, in the operation of fracturing pump equipment, it is recommended to use full-thread structure bolts.

Author Contributions: Conceptualization, H.L.; investigation, H.L. and X.W.; supervision, R.S. and X.W.; visualization, Y.W. and X.S.; writing—original draft, H.L.; writing—review and editing, W.T. and B.W. All authors have read and agreed to the published version of the manuscript.

Funding: This work was financially supported by the National Natural Science Foundation of China (No. 52105456).

Data Availability Statement: The data is unavailable due to privacy.

Conflicts of Interest: The authors declare no conflict of interest.

References

1. Zhang, R.L.; Zheng, X.S.; Li, S.R.; Jin, K.; Zheng, H.J.; Wang, L. Environmentally friendly hydraulic fracturing and water-free fracturing technologies. *Int. J. Oil Gas Coal Technol.* **2018**, *17*, 375–390. [CrossRef]
2. Zhao, M.Y. Field experiments and main understanding of shale oil hydraulic fracturing. *Front. Earth Sci.* **2024**, *12*, 1410524. [CrossRef]
3. Yu, D.W.; Tan, L.J.; Shi, X.J. Development Trend and Key Technologies of Hydraulic End of High-Power Fracturing Pump. *China Pet. Mach.* **2024**, *52*, 118–123.
4. Sun, C.; Zheng, H.; Liu, W.D.; Lu, W.T. Numerical investigation of complex fracture network creation by cyclic pumping. *Eng. Fract. Mech.* **2020**, *233*, 107103. [CrossRef]
5. He, X.; Liu, Q.Y.; Zhao, M.; Zhao, Y.; Tian, J.Y. Fatigue prediction for pump end of high pressure fracturing pump. *Adv. Mater. Res.* **2011**, *337*, 81–86. [CrossRef]
6. Kiani, M.; Walker, R.; Babaeidarabad, S. Numerical Modeling and Analytical Investigation of Autofrettage Process on the Fluid End Module of Fracture Pumps. *J. Press. Vessel. Technol.* **2018**, *140*, 041403. [CrossRef]
7. Wei, C.; Zhou, S.Z.; Li, M.Q.; Zhang, S. Numerical investigation on fatigue crack growth of fracturing pump head using cohesive zone model. *Theor. Appl. Fract. Mech.* **2020**, *107*, 102564. [CrossRef]
8. Zhang, S.; Zhou, S.Z.; Li, M.Q. Research on fatigue crack propagation process of fracturing pumphead. *Eng. Fail. Anal.* **2020**, *116*, 104726. [CrossRef]
9. Hu, G.; Deng, S.Y.; Wang, G.R.; Wang, M.C.; Xie, M.Y. Corrosion crack's propagation analysis and fatigue life prediction of the cylinder of 6000HP hydraulic fracturing pump. *Eng. Fail. Anal.* **2022**, *141*, 106652. [CrossRef]
10. Pedrosa, B.; Rebelo, C.; Gervásio, H.; da Silva, L.S.; Correia, J.A. Fatigue of preloaded bolted connections with injection bolts. *Struct. Eng. Int.* **2020**, *30*, 102–108. [CrossRef]
11. Ajaei, B.B.; Soyoz, S. Effects of preload deficiency on fatigue demands of wind turbine tower bolts. *J. Constr. Steel Res.* **2020**, *166*, 105933. [CrossRef]
12. Yang, L.; Yang, B.; Yang, G.W.; Jiang, L.X.; Xiao, S.E.; Zhu, T. Fatigue evaluation method based on equivalent structural stress approach for bolted connections. *Int. J. Fatigue* **2023**, *174*, 107738. [CrossRef]
13. Yang, L.; Yang, G.W.; Zhang, Z.; Yuan, Y.Q.; Kang, G.Z. Fatigue life prediction method for bolted joints based on equivalent structural stress under tensile–compressive loading. *Int. J. Fatigue* **2025**, *190*, 108625. [CrossRef]
14. Zhang, W.Y.; Xie, J.Y.; Li, T.X.; Ding, Y.K. Tensile low-cycle fatigue performance and life prediction of high-strength bolts. *J. Constr. Steel Res.* **2022**, *197*, 107468. [CrossRef]
15. Kopei, V.B.; Onysko, O.R.; Kopei, I.B.; Panchuk, V.G.; Bukatka, Y.S.; Goroshko, A.V. Influence of mechanical characteristics of materials of threaded connections of oil and gas downhole equipment on their fatigue life. *J. Phys. Conf. Ser.* **2024**, *2927*, 012014. [CrossRef]
16. Yu, Q.M.; Zhou, H.L.; Yu, X.D.; Yang, X.J. High-temperature low cycle fatigue life prediction and experimental research of pre-tightened bolts. *Metals* **2018**, *8*, 828. [CrossRef]
17. Mrówczyński, D.; Gajewski, T.; Garbowski, T. Parametric Study of the Numerical Model of a Bolted Connection of Steel Structure for Photovoltaic Panels. *Materials* **2022**, *15*, 6794. [CrossRef]
18. Okorn, I.; Nagode, M.; Klemenc, J.; Oman, S. Analysis of additional load and fatigue life of preloaded bolts in a flange joint considering a bolt bending load. *Metals* **2021**, *11*, 449. [CrossRef]
19. Yao, S.G.; Zhang, M. Effect of preload on tensile fracture of variable cross-section bolts: Experiment and simulation. *Metals* **2023**, *13*, 744. [CrossRef]
20. Jia, J.F.; Yu, X.L.; Zhang, X.Y.; Lv, Q.; Ye, J.C. Bolt body axial stress detection based on nut axial stress. *J. Constr. Steel Res.* **2023**, *211*, 108190. [CrossRef]
21. Cruces, A.S.; Garcia-Gonzalez, A.; Moreno, B.; Itoh, T.; Lopez-Crespo, P. Critical plane based method for multiaxial fatigue analysis of 316 stainless steel. *Theor. Appl. Fract. Mech.* **2022**, *118*, 103273. [CrossRef]
22. Liu, J.H.; Zhang, Z.; Li, B.; Lang, S.S. Multiaxial fatigue life prediction of GH4169 alloy based on the critical plane method. *Metals* **2019**, *9*, 255. [CrossRef]
23. Brown, M.W.; Miller, K.J. A theory of fatigue under multiaxial stress-strain conditions. *Proc. Inst. Mech. Eng.* **1973**, *187*, 745–755. [CrossRef]
24. Portugal, I.; Olave, M.; Urresti, I.; Zurutuza, A.; López, A.; Muñiz-Calvente, M.; Fernández-Canteli, A. A comparative analysis of multiaxial fatigue models under random loading. *Eng. Struct.* **2019**, *182*, 112–122. [CrossRef]
25. Yang, H.Z.; Ding, J.H.; Li, Q.Q.; Li, H.J. Multiaxial fatigue analysis on reeled deepwater steel catenary risers with girth weld defects. *China Ocean Eng.* **2014**, *28*, 857–868. [CrossRef]
26. Song, D.D.; Wang, T.Q.; Zhu, S.; Liu, Z.J. Extrapolation Framework and Characteristic Analysis of Load Spectrum for Agriculture General Power Machinery. *Processes* **2024**, *12*, 2078. [CrossRef]

27. Colin, B. Stochastic approach of fatigue vibratory: Comparison between Peak-Valley method and rainflow counting method. *Rev. Metall.* **2012**, *109*, 217–247. [CrossRef]
28. *DASt-Guideline 021: Schraubenverbindungen aus Feuerverzinkten Garnituren M39 Bis 72*; Deutscher Ausschuss für Stahlbau DASt, Stahlbau Verlags- und Service GmbH: Düsseldorf, Germany, 2013.

Disclaimer/Publisher's Note: The statements, opinions and data contained in all publications are solely those of the individual author(s) and contributor(s) and not of MDPI and/or the editor(s). MDPI and/or the editor(s) disclaim responsibility for any injury to people or property resulting from any ideas, methods, instructions or products referred to in the content.